Application of Wireless Sensor Network in Rock Bolt Pulling Force Distribution Pattern Monitoring

Application of Wireless Sensor Network in Rock Bolt Pulling Force Distribution Pattern Monitoring

Zhuo Yang[1,2], **Wenxiang Peng**[3*], **Jiaqiang Cao**[4], **Ding Xie**[5]

[1]Guangzhou Institute of Building Science CO., LTD., Guangzhou 510440, China
[2]School of Civil Engineering, Guangzhou University, Guangzhou 510006, China
[3]School of Earth Sciences and Information Physics, Central South University, changsha 410000, China
[4]Guangzhou Construction Engineering Quality and Safety Testing Center Co., Ltd., Guangzhou 510006, China
[5]Guangzhou Institute of Building Science, New Technology Development Center Co., Ltd.,
Guangzhou 510006, China
*Corresponding author email:165503593@qq.com

Abstract. The application of rock bolting in the reinforcement of underground engineering and tunnel engineering is becoming more extensive, and the stress distribution pattern of rock bolt is a necessary means for quality monitoring. To investigate the stress characteristics of the rock bolt during usage, this paper tests the stress and strain changes of the full-length anchoring rock bolt and the end anchoring rock bolt under the action of pulling force based on the wireless sensor network (WSN) technology, it analyzes the strain characteristics of the exterior of the rock bolt. The research shows that the axial force of the full-length anchoring rock bolt increased with the increase of the load, when the load reached 28MPa, the bolt at the end of rock bolt rod slid; the longitudinal strain of the base of the end anchoring rock bolt was only affected by the top pressure, the shear stress of the middle hollow anchoring section was 0, and the axial strain was the largest; for the full-length anchoring rock bolt, the shear stress was distributed along the whole length of the rod body, and the strain value at the front end was the largest; for the two anchoring methods, both the wavelength drift of the fiber Bragg grating (FBG) measuring points on the rod body of rock bolt and the strain of the base increased with the increase of the load. This study lays a theoretical foundation for long-term quality monitoring and evaluation of rock bolting based on WSN.

1. Introduction

With the rapid development of scientific technology and industrial techniques, the yield of coal resources is also increasing year by year, and along with the development of the coal industry, there appear more issues concerning miners and property safety in the coal mining process. The investigation found that one of the causes of coal mine accidents was that the roadway support did not meet the requirements or the support was insufficient [1-3]. The rock bolting technique has the advantages of high efficiency, low cost and safety, and it has been applied more and more in the engineering field [4,5]. Most coal mines use rock bolting technique for geotechnical engineering reinforcement [6,7]. Rock bolting is a concealed project. In the process of engineering reinforcement, the quality of the rock bolt needs to be monitored. The stress state of the rock bolt is quite complicated, using effective monitoring method to investigate the internal force distribution of the rock bolt [8-10].

Wireless grating sensors are a new type of WSN technology that has been applied to underground and tunnel engineering in recent years. FBG sensor is one of the most commonly used sensing technologies, it has the multiplexing capability of sensing and data transmission [11,12]. As a sensitive component, it can directly sense and measure the strain and temperature, as well as other relevant physical and chemical quantities [13,14]. Applying WSN technology to measure the stress distribution pattern of rock bolting in coal mines and other underground engineering projects is of important theoretical significance and social value.

Based on current rock bolting reinforcement technology and wireless sensing technology, through the axial pull-out test of rock bolt, this paper uses wireless sensors to monitor the stress status of the rock bolt, analyzes the strain characteristics of the outer part of the base and the stress distribution pattern of the rock bolt rod body, so as to monitor the quality of the rock bolt under different anchoring status.

2. Rock bolt pull-out test

2.1Test piece fabrication

In this paper, two model test pieces were fabricated, one of which was used for the full-length anchoring rock bolt pull-out test, and the other was used for the end anchoring rock bolt pull-out test. The test piece is consisted of two parts: the base and the rod. The size of the base model was 300mm in diameter and 1100mm in height. The materials were 32.5R common Portland cement, standard sand, with water as the mixture. The ratio of sand, cement and water was 1:1:0.5, three cubic test pieces were fabricated for mechanical property test, the data obtained from compression test are shown in Table 1. In the test, the compressive strength of the test block was 31.5 MPa, and the corresponding compressive strength of the simulated sandstone was 44.3 MPa, therefore, sandstone was used to simulate the actual rock mass in the coal mine. After the casting of the base model was completed, after 28 days of curing, the rock bolts were installed in the reserved holes to complete the fabrication of the test pieces. The process for installing rock bolt with full-length anchoring was: filling resin cartridge into the preserved hole → installing rock bolt → sealing the hole; the process for installing rock bolt with end anchoring was: installing the expansion shell → applying prestress.

Table 1. Data of compressive test pieces

Serial number	Compressive strength/MPa	Modulus of elasticity/MPa	Poisson ratio
1	33.1	0.81×105	0.23
2	29.3	0.77×105	0.19
3	32.2	0.92×105	0.22
average	31.5	0.85×105	0.21

2.2Rock bolt monitoring

See Figure 1 for the arrangement of BFG on the rock bolt, the three gratings of the full-length anchoring were evenly distributed on the rod body with a spacing of 300 mm and were strung together, the center wavelength was 1532 nm, 1527 nm, and 1525 nm, respectively; the spacing of FBG of end anchoring was 300mm, it's a separate fiber, and the center wavelength was 1554nm, 1562nm, and 1561nm, respectively. The spacing between each set of strain gauge (including the lateral direction and the longitudinal direction) was 150 mm, and the position of the strain gauges was 120 mm, 270 mm, 420 mm, 570 mm, and 720 mm from the top, respectively.

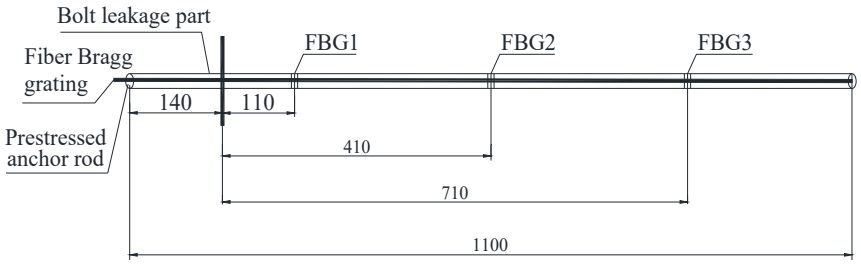

(a) FBG arrangement on full-length anchoring rock bolt

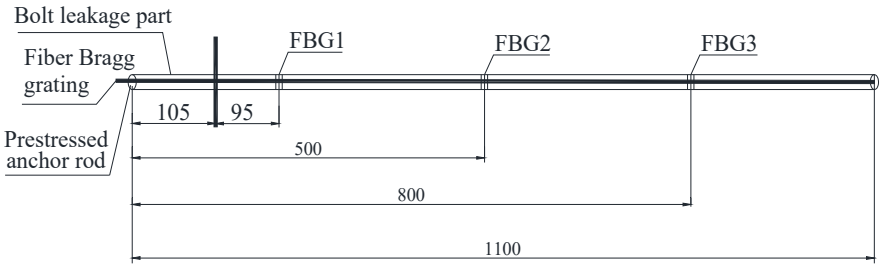

(b) FBG arrangement on end anchoring rock bolt
Figure 1. FBG arrangement of the rod body

3. Stress distribution pattern of rock bolt and quality inspection

By linear fitting, the relationship between the wavelength shift amount λ of the sensor in the grating rock bolt and the load F was obtained, as shown in Equation 1.

$$F = \mathbf{84.87} \times \Delta\lambda + \mathbf{4.45} \tag{1}$$

Where: Δλ is the wavelength shift (nm) of the FBG sensor; F is the external load (kN) during the loading process of rock bolt.

3.1Full-length anchoring

In the loading process of FBG rock bolt, the stress of the rod and the load at the bolt head of the rock bolt were calculated by Equation 1, as shown in Table 2. It can be seen that when the stress of the rock bolt reached 28 MPa, the load at the bolt head of the rock bolt reached a maximum value of 79.98 kN, after the loading was continued, the stress of the rock bolt was disabled, when the loading was applied for the 15th time, the load at the bolt head of the rock bolt was reduced to 70.12kN. According to Equation 2, we can calculate to get the initial wavelength dλB of FBG1, FBG2 and FBG3, and thereby calculating to get the corresponding strain sensitivity coefficient Kε as 1.1974, 1.1935 and 1.1896, respectively, and finally obtain the strain value of the three sensors' corresponding positions (110mm, 410mm and 710mm in turn), the variation of the strain value of the rod under different loads is shown in Figure 2. It can be seen from Figure 2 that the strain at three positions of the full-length anchoring rock bolt gradually increased with the increase of the load. The strain value at FBG1 was the largest and the increasing trend was the most obvious, indicating that the strain value at the front end of the full-length anchoring rock bolt was relatively large.

$$d\lambda_B = K_\varepsilon \varepsilon_z ,\ K_\varepsilon = (\mathbf{1} - P_e)\lambda_B \tag{2}$$

Table 2. Load measured by bolt dynamometer under different loads

Loading times	Load /MPa	Wavelength shift/pm	Load of anchor head /kN	Loading times	Load /MPa	Wavelength shift/pm	Load of anchor head /kN
0	0	0	0	6	14	479	45.12

1	2.5	115	14.15	8	18	599	55.27
2	5	183	19.95	10	22	728	66.22
3	8	268	27.04	12	26	852	76.91
4	10	336	32.94	13	30	901	79.98

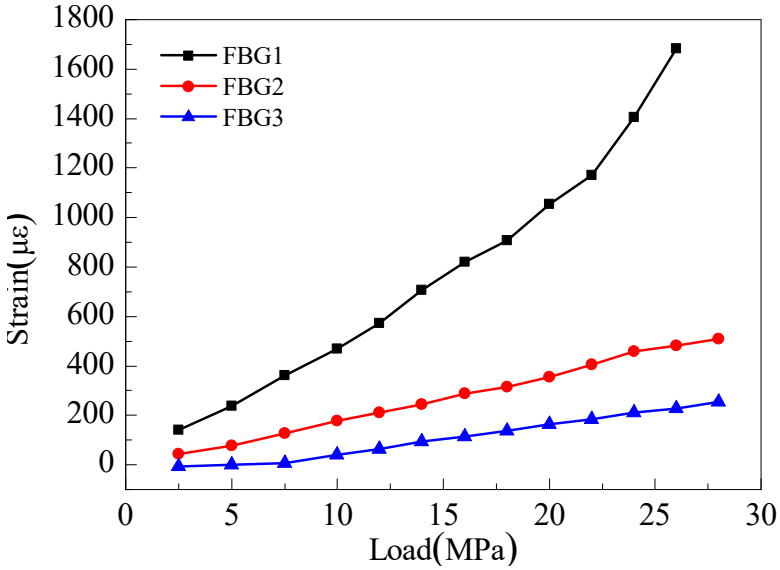

Figure 2. Strain of rock bolt under different loads

According to the rock bolt strain data measured by FBG, the axial force of the rock bolt was obtained, and the axial force distribution pattern of the rock bolt under different loads was obtained, as shown in Figure 3. It can be seen that the axial force of the rod increased continuously with the increase of the load. When loading was applied for the 13th time, the axial stress reached 28MPa, the bolt at the end of the rock bolt slid, the FBG1 exceeded the measuring range, and the full-length anchoring rock bolt failed.

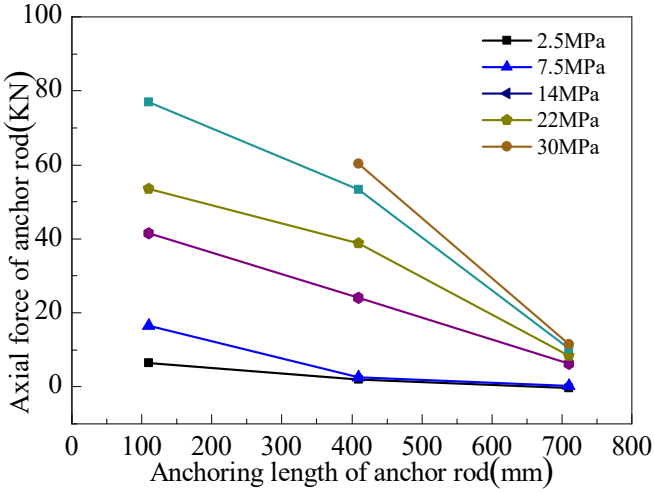

Figure 3. Strain of rock bolt under different loads

3.2 End anchoring

In the loading process of end anchoring rock bolt, the stress of the rod and the load at the bolt head of the rock bolt are shown in Table 3. It can be seen that when the loading was applied for the 8th time, namely the stress of the rock bolt reached 18 MPa, the load at the bolt head of the rock bolt reached a maximum value of 60.8 kN. According to Equation 2, the initial wavelengths $d\lambda_B$ of FBG1, FBG2 and FBG3 of the end anchoring rock bolt were calculated, and the corresponding strain sensitivity

coefficient K_ε was calculated to be 1.2130, 1.2192 and 1.2185 respectively, finally, the distance of the three fiber grating sensors of FBG1, FBG2 and FBG3 was obtained to be 200mm, 500mcm and 800mm from the top of the rock bolt, respectively.

Table 3.Load on FBG anchor dynamometer under different loads

Loading times	Load/ MPa	Wavelength drift/MPa	Anchor head load/kN
0	0	0	0
1	2.5	75.7	10.9
2	5	281.3	28.3
3	7.5	332.9	32.6
4	10	412.8	39.5
5	14	534.7	49.9
6	18	662.9	60.8

According to the different positions of measuring points and the change of the load, the FBG strain change pattern of each measuring points under different loads can be obtained. As shown in Figure 4, as the load increased, the strains of all three measuring points gradually increased, and the amount of change was approximately the same. All three measuring points of FBG1, FBG2 and FBG3 were located in the hollow anchoring section of the end anchoring, so the strain generated during the stressing process of the rock bolt changed uniformly

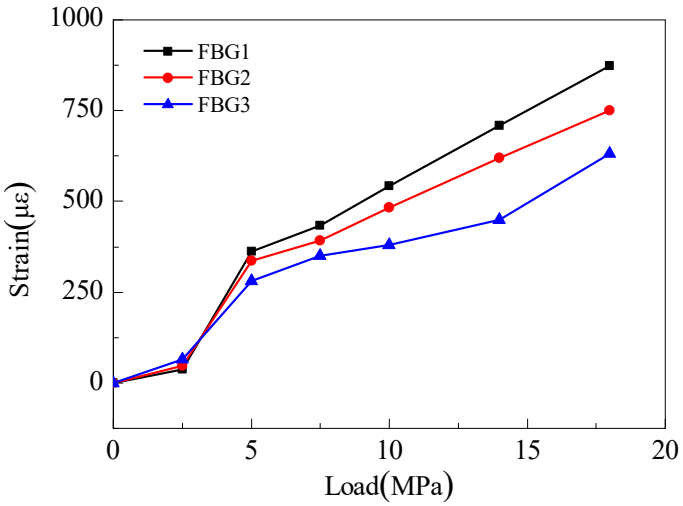

Figure 4.Strain variation of FBG measuring points under different loads

4. Conclusion

Based on the existing rock bolting reinforcement technology and wireless sensor network, this paper designed an axial pull-out test for the rock bolt, and used the wireless sensor network to monitor the stress of the rock bolt, it analyzed the strain characteristics of the outer part of the base of the rock bolt under the pulling force. The main conclusions are as follows:

(1) For the two anchoring methods, both the wavelength drift of the measuring points on the rock bolt rod body and the strain change of the base gradually increased with the increase of the load.

(2)For the full-length anchoring rock bolt, when the load was applied for the 13th time, and end of the rod slid, that is, when the stress reached 28MPa, the rock bolt was disabled; the axial force of the rock bolt increased with the increase of external load, when the load was applied, the shear stress was distributed along the full-length of the rock bolt, and the maximum strain of the rod appeared at the front end.

(3) For the end anchoring rock bolt, the axial strain of the outer part of the base increased with the increase of the load, and the strain distribution of the anchoring section was not uniform; the stress distribution of the middle hollow anchoring section of the end anchoring rock bolt was uniform, and

there was no shear stress, the maximum strain of the rock bolt rod body appeared in the middle of the rod body.

Acknowledgment
The authors acknowledge the financial support from Guangzhou Science Technology and Innovation Commission (201803030009) and National Natural Science Foundation (51678171).

References

[1] Tang X J, Qi D, Sun T, Wu J and Yang X G 2010 *International Conference on Wireless Communications Networking & Mobile Computing, IEEE Xplore*.**10** 1.
[2] Martinez J, Sisman A, Onen O, Velasquez D and Guldiken R 2012 *Sensors*, **12** 12265.
[3] Zangaro R A, Silveira L J, Barreto da S R 1994 *International Conference on Vibration Measurements by Laser Techniques: Advances & Applications. International Society for Optics and Photonics*. **2358** 333.
[4] Yang S , Wang Z , Jiang H , Wang Z Y and Liu H 2016 *Electronics Letters*, **52** 1660-1661.
[5] Shinoda H and Oasa H 2000 *IEEE/ASME Trans on Mechatronics*. **5** 258.
[6] Liu S , Li Y , Wang T and Luo Y 2014 *Sensor Review*. **34** 337.
[7] Peng F , Ji H G and Yan X Z 2012 *Applied Mechanics and Materials*. **178** 4.
[8] Ho S C M , Li W , Wang B and Song G B 2017 *Smart Materials and Structures*. **26** 1.
[9] Etse G 1998 *Nuclear Engineering & Design*. **179** 245 .
[10] Kondo G and Morita S 1992 *Journal of Structural & Construction Engineering*. **24** 141 .
[11] Park J H , Hong D S , Kim J T , Koo K Y , Yun C B and Park G 2008 *Advances in Science & Technology*. **56** 420.
[12] Park J , Kim J , Hong D , Mascarenas D and Peter Lynch J 2010 *Smart Structures & Systems*. **6** 711 .
[13] Olivera J , González M , Fuente J V , Varga R , Zhukov A and Anaya J J 2014 *Sensors*. **14** 19963 .
[14] Butler L J , Gibbons N, He P, Middleton C and Elshafie M Z E B 2016 *Construction & Building Materials*. **126** 894 .